

First-principles Study on the Atomic and the Electronic Structures of Unreconstructed 6H-SiC{0001} Surfaces and Epitaxial Graphene

Seungchul KIM and Jisoon IHM

Department of Physics and Astronomy, Seoul National University, Seoul 151-747

Young-Woo SON*

Department of Physics, Konkuk University, Seoul 120-749

(Received 26 August 2008)

We present an *ab initio* study on the structural and electronic properties of {0001}-(1 × 1) surfaces of 6H-SiC and of epitaxial graphene on top of the surfaces, respectively. The fully-relaxed structure of the Si-terminated (0001) surface is found to be almost identical to the sp^3 bonding geometry of the bulk 6H-SiC while that of the C-terminated (000 $\bar{1}$) side is flattened to have mixed characteristics of sp^3 and sp^2 bondings. Both surfaces have ferromagnetically-ordered surface states with indirect band gaps. When graphene is commensurately placed on top of the SiC{0001}-(1 × 1) surfaces, it opens a wide energy gap at the Dirac point owing to strong covalent bondings to the SiC surface and, thus, forms an insulating buffer layer. Graphene on top of the buffer layer is shown to have linear energy bands and to exhibit a very small energy gap at the Dirac point due to sublattice-symmetry-broken interactions between the buffer layer and graphene.

PACS numbers: 73.20.-r, 68.35.-p, 71.20.-b, 81.05.Uw

Keywords: SiC, Epitaxial graphene, Surface state, Ferromagnetism

I. INTRODUCTION

Recent successes in isolating graphene—a single layer of graphite [1–3]—have attracted the notice of many researchers from various disciplines due to its interesting physical properties and its potential applications [4, 5]. One approach to fabricating graphene on semiconductors is to heat hexagonal silicon carbide (*H*-SiC) with specific surfaces up to very high temperatures [6–9]. Then, graphene can grow epitaxially on either the silicon-terminated (0001) or the carbon-terminated (000 $\bar{1}$) surface of 4H-SiC and 6H-SiC, respectively [6, 7]. Low-energy electrons in epitaxial graphene satisfy the relativistic energy-momentum dispersion described by the Dirac Hamiltonian [6–9], being similar to those in mechanically exfoliated graphene [2, 3]. Interestingly, several works have shown that the physical properties of epitaxial graphene and the underlying structures on the (0001) surface are different from those on the (000 $\bar{1}$) surface [6–15]. Moreover, modifications of electronic structures occur at the Dirac point of graphene on the (0001) surface [8, 9, 12].

On the other hand, long before graphene research, the

physical properties of reconstructed surfaces of *H*-SiC had been studied extensively [16–25]. Without heating to very high temperature, unlike the case of epitaxial graphene, both the (0001) and the (000 $\bar{1}$) sides of *H*-SiC were observed to undergo various reconstructions, *e.g.*, $\sqrt{3} \times \sqrt{3}$, 3×3 and $\sqrt{3} \times \sqrt{3}R30^\circ$ times the unit cell of the surfaces [16–18]. Notably, the $\sqrt{3} \times \sqrt{3}R30^\circ$ reconstructed 6H-SiC (0001) surface is known to be a Mott-Hubbard insulator [22]. The unreconstructed surface is believed to be unstable because its chemically active surface can be easily reconstructed by additional atoms (including oxidation). However, the unreconstructed 1 × 1 surface of 6H-SiC was observed recently, and its electronic structures were analyzed by using angle-resolved photoemission spectroscopy measurements [24, 26]. The unreconstructed *H*-SiC surfaces have unsaturated *p*-orbitals of Si or C so that there may be a possible ferromagnetic ordering at the surface. We notice that various magnetic orderings can occur in other organic materials without *d*- or *f*-orbitals [27–37].

In consideration of the aforementioned interests in graphene and the magnetic ordering at the unreconstructed SiC surface, it is important to understand the similarities and the differences in the physical properties between unreconstructed Si- and C-terminated surfaces of *H*-SiC{0001} directions. It is also necessary to explore the atomic and the electronic structures of epi-

*Corresponding Author: hand@kias.re.kr;

Present Address: Korea Institute for Advanced Study, Seoul 130-722

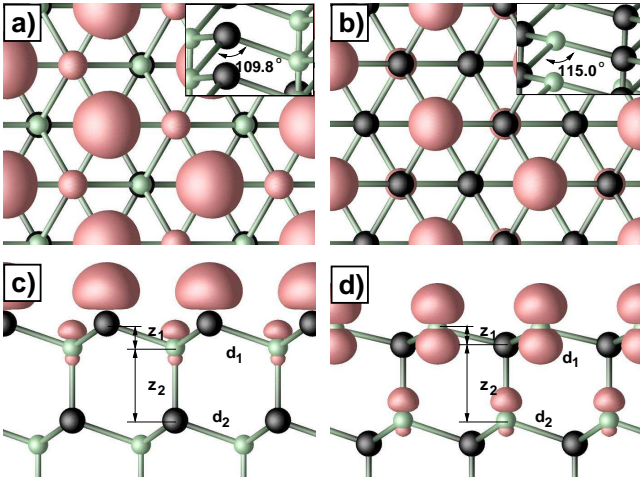


Fig. 1. Top [(a) and (b)] and side [(c) and (d)] views of the ground state atomic geometries and spin-polarized surface states of $6H$ -SiC(0001) [(a) and (c)] and (000 $\bar{1}$) [(b) and (d)] directions, respectively. Green and black balls indicate carbon and silicon atoms, respectively. The squared amplitudes of the wavefunctions (isosurface of 0.1 \AA^{-3}) of the spin-polarized surface state on both sides are drawn. Insets in (a) and (b) show the bonding angle of the surface atoms. In (c), $z_1 = 0.62 \text{ \AA}$, $z_2 = 1.89 \text{ \AA}$, $d_1 = 1.88 \text{ \AA}$ and $d_2 = 1.88 \text{ \AA}$. In (d), $z_1 = 0.41 \text{ \AA}$, $z_2 = 1.95 \text{ \AA}$, $d_1 = 1.82 \text{ \AA}$ and $d_2 = 1.88 \text{ \AA}$.

taxial graphene on top of both surfaces to understand the experimental findings [6–9, 13–15]. In this paper, we present first-principles calculation results on the electronic and the geometric structures of the $6H$ -SiC(0001) and (000 $\bar{1}$)-(1 \times 1) surfaces and on epitaxial graphene on top of them. Specially, epitaxial graphene is placed commensurately on top of the $6H$ -SiC{0001} surfaces to reduce the computational complexity.

II. SIMULATION METHOD

We carried out first-principles calculations using localized pseudo-atomic orbital (PAO) basis sets [38] based on the density functional theory within the local spin density approximation (LSDA) by employing the Perdew-Zunger parametrization [39] of the Ceperley-Alder exchange-correlation energy functional [40]. Norm-conserving pseudopotentials [41] were used with the Kleinman-Bylander's fully separable nonlocal projectors [42]. The double- ζ plus polarization PAO basis set [38] was used for all atoms in the calculations. A uniform k -point sampling of 12×12 points was employed for all configurations considered in the paper. The energy cutoff for a real space mesh size was 300 Rydberg. All geometries were fully relaxed until the forces on each atom were less than 0.01 eV/\AA . We adopted a slab geometry to explore surface states and epitaxial graphene and found that 6 layers of Si and C atoms were enough to avoid interactions between opposite sides of

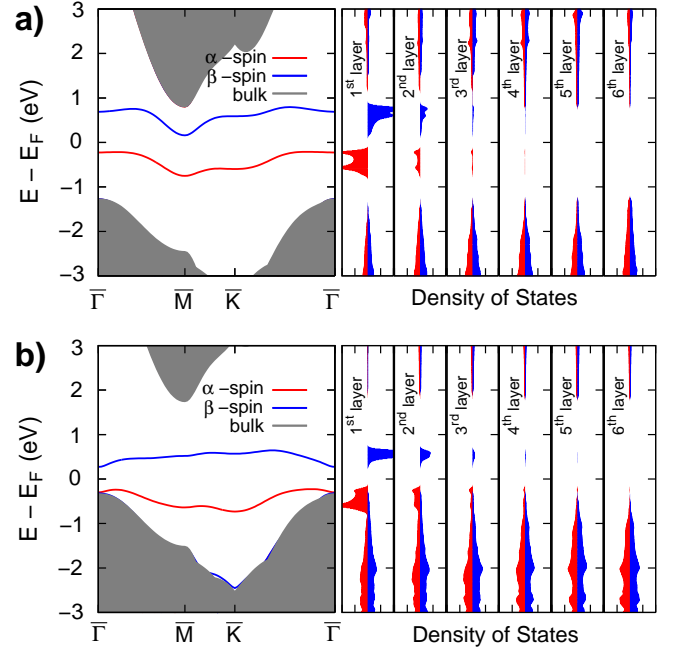


Fig. 2. Band structures (left panels) and projected density of states (right panels) on each layer of the (a) $6H$ -SiC(0001) surface and the (b) (000 $\bar{1}$) surface. The Fermi energy (E_F) of each panel is set to zero.

the slab. The opposite side of a surface of interest was passivated by using hydrogen atoms. Without adatoms on the surfaces, we performed relaxations of both surfaces with 2×2 , $\sqrt{3} \times \sqrt{3}$, and 3×3 times the surface unit cell but did not find any reconstruction.

III. RESULTS

1. Unreconstructed $6H$ -SiC{0001} Surfaces

The fully relaxed ground state configuration of the (0001) surface (Figs. 1(a) and (c)) has an atomic structure very similar to that of the truncated bulk without reconstructions. The angle between covalent bonds of Si and C at the surface is 109.8° (inset in Fig. 1(a)), which is almost identical to the case of ideal sp^3 covalent bonding (109.5°). Likewise, the bonding length of the Si-C covalent bond at the surface (d_1 in Fig. 1(c)) and of that in the second layer (d_2 in Fig. 1(c)) are the same as the bulk value (1.88 \AA). All other geometrical parameters (z_1 and z_2 in Fig. 1(c)) also indicate that the atomic structure of the $6H$ -SiC(0001) surface remains the same with respect to the bulk structure if the surface maintains 1×1 periodicity. The optimized geometry of the (000 $\bar{1}$) direction, however, is quite different from the atomic structure of the (0001) surface and the bulk. When the carbon-terminated (000 $\bar{1}$) surface is exposed to vacuum, the foremost layer of carbons is flattened and has the mixed bonding characteristics of sp^2

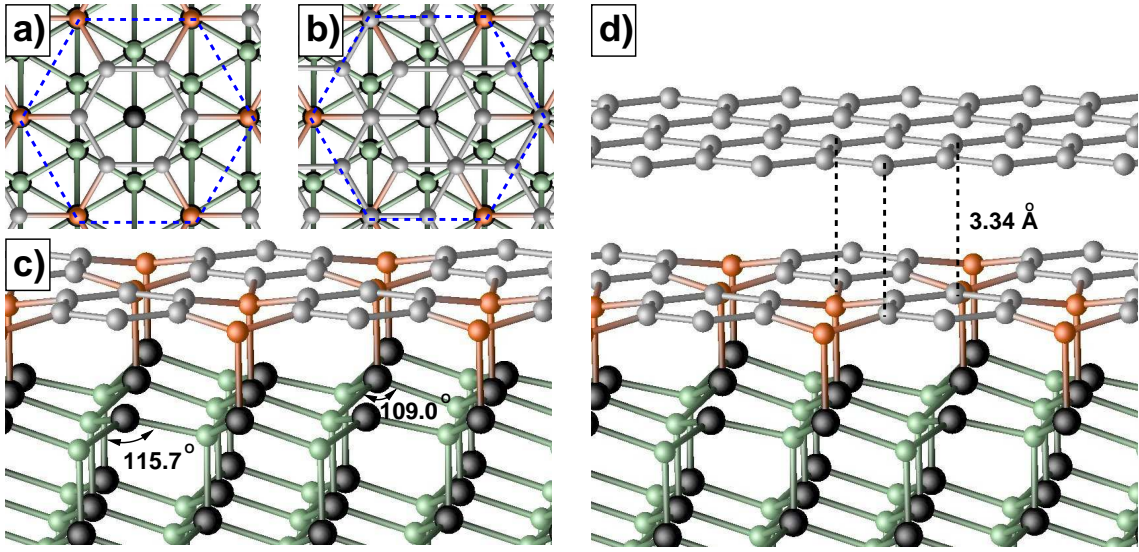


Fig. 3. Top [(a) and (b)] and side [(c) and (d)] views of the ground state atomic geometries of the buffer layer [(a) and (c)] and of epitaxial graphene [(b) and (d)] with $\sqrt{3} \times \sqrt{3}R30^\circ$ periodicity, respectively. Green and black balls indicate carbon and silicon atoms, respectively. The dotted blue lines in (a) and (b) denote an unit cell of $\sqrt{3} \times \sqrt{3}R30^\circ$ periodicity. Gray and orange balls indicate carbon atoms in the buffer layer and graphene with and without covalent bonding to silicon atoms underneath them, respectively.

and sp^3 hybridizations of $2s$ - and $2p$ -orbitals. The angle between the covalent bonds of C and Si at the $(000\bar{1})$ surface is 115.0° (inset in Fig. 1(b)), which is almost an average value between the 120° of sp^2 bonding and the 109.5° of sp^3 bonding.

We find that, for both surface directions, the ferromagnetic surface state is favored over other possible magnetic orderings and over the paramagnetic state. The unsaturated dangling bonds of silicon (carbon) atoms on the (0001) [$(000\bar{1})$] surface are weakly interacting with each other due to large spacing (3.08 \AA) between them, so without consideration of the spin degree of freedom in electrons, they form a half-filled surface band with a narrow band width, which can be spin-polarized eventually. The total energy difference between the semiconducting ground state and the paramagnetic metallic state is 0.11 eV (0.22 eV) per unit cell for the case of the $6H\text{-SiC}(0001)$ [$(000\bar{1})$] surface. We find that the spin-polarized states are located at the topmost layer of the systems (Figs. 1(c) and (d)) and that the projected spin-polarized density of states rapidly decreases to zero as getting into the bulk (Figs. 2(a) and (b)), implying non-spin-polarized bulk states.

We also find that, for the (0001) [$(000\bar{1})$] side, an antiferromagnetic ordering of the surface states have a slightly higher total energy of 20 meV (30 meV) per unit cell compared with the ground ferromagnetic states. The antiferromagnetic states for both surfaces are also semiconducting with similar gap sizes, but with reduced band widths for conduction and valence surface bands, compared with those of the ferromagnetic states (not shown here).

2. Commensurate Epitaxial Graphene

To calculate the atomic and the electronic structures, we place a single layer of graphene on the unreconstructed $6H\text{-SiC}\{0001\}$ surface commensurately. In order to maintain the minimal size of the common unit cell between graphene and the SiC surface, we elongate the lattice constant of graphene by $\sim 8\%$ (Figs. 3(a) and (c)). The final commensurate common unit cell for calculations is $\sqrt{3} \times \sqrt{3}R30^\circ$ times the surface unit cell of the $6H\text{-SiC}\{0001\}$ surface. The same atomic geometry was also used in previous studies [10,11]. We note that the actual minimal commensurate common cell between graphene and the $6H\text{-SiC}\{0001\}$ surface is much larger than the one adopted in the present study. It corresponds to 13×13 times the unit cell of graphene and $6\sqrt{3} \times 6\sqrt{3}R30^\circ$ times the unit cell of the $6H\text{-SiC}\{0001\}$ surface [9–13].

When graphene is on the silicon-terminated $6H\text{-SiC}\{0001\}$ - (1×1) surface with $\sqrt{3} \times \sqrt{3}R30^\circ$ periodicity, some of carbon atoms in graphene (denoted by orange in Fig. 3(c)) have strong covalent bonds to the surface. The bond length between carbon in graphene and silicon on the surface is 2.00 \AA . The surface silicon atoms with covalent bondings to carbon atoms in graphene have sp^3 bonding configurations (see Fig. 3(c)) while ones without covalent bondings have the mixed characteristics of sp^3 and sp^2 bondings (Fig. 3(c)). When we put another layer of graphene on top of the previous structure (the unit cell of graphene here is also elongated as much as the one before), the resulting graphene does not show any vertical corrugations, and the interlayer

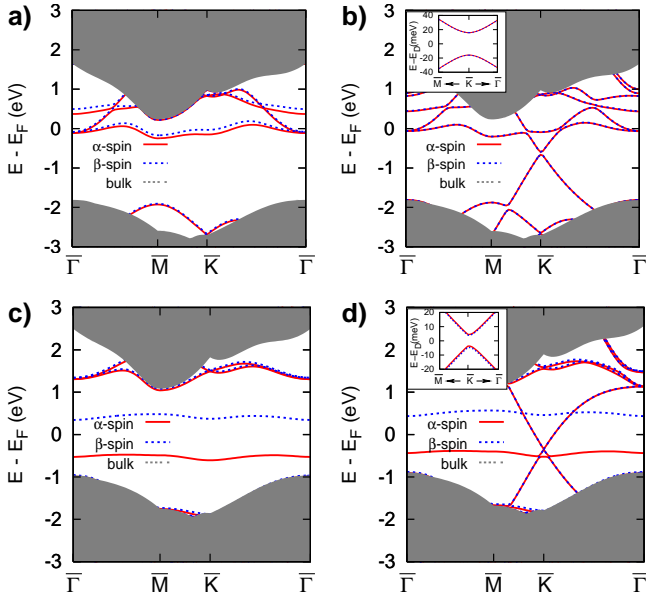


Fig. 4. Band structures of (a) a buffer layer on $6H$ -SiC(0001) [atomic geometry shown in Fig. 3(c)] and of (b) graphene on top of the buffer [Fig. 3(d)]. Corresponding band structures for the $6H$ -SiC(0001) direction are in (c) and (d). The Fermi energy (E_F) of each panel is set to zero. The insets in (b) and (d) are enlarged band structures near the Dirac point at \bar{K} . The energy of the Dirac point (E_D) is assumed to be the center of the small gap and is set to zero.

distance between two graphenes is 3.34 \AA (Fig. 3(d)). Similar calculation results are obtained for the model epitaxial graphene with $\sqrt{3} \times \sqrt{3}R30^\circ$ periodicity on the carbon-terminated $6H$ -SiC(0001)-(1 \times 1) surface (not shown here).

When graphene has selective covalent bonds to the surface, the hexagonal network of π -electrons of graphene is broken so that the characteristic linear band disappears (Fig. 4(a)). Instead, we find the almost flat bands near the Fermi energy (E_F) with a large energy gap ($\sim 2 \text{ eV}$). We also find that the states are slightly spin-polarized due to aforementioned surface spin-polarizations, so the semiconducting graphene on the surface indicates that the first graphene layer on the SiC surface forms a buffer layer [6–13]. The buffer layer on the (0001) surface shows a similar semiconducting behavior, but the energy gap ($\sim 1 \text{ eV}$) is smaller than one on the (0001) side (Fig. 4(c)). We note that similar calculation results were obtained in previous studies [10,11]. It is notable that the buffer layer on this side is completely spin-polarized, as shown in Fig. 4(c).

When graphene is commensurately placed on top of both buffer layers, it maintains the characteristic linear energy bands near the Dirac point (E_D) and is shown to be electron doped (Figs. 4(b) and (d)). Detailed electronic structures near the E_D , however, show minute gaps at the E_D of the linear energy bands, as shown in the insets of Figs. 4(b) and (d), respectively. Due to

alternating surface corrugations and covalent bondings of the buffer layer, each sublattice of graphene experiences a small difference in interactions with the underlying buffer layer. The resulting broken symmetry between the two sublattices of graphene can induce a gap at the E_D of each system [4,9,12]. The size of the gap for graphene on the (0001)[(0001)] side is 30 (10) meV, which is quite small compared with values (200 \sim 240 meV) from experiments [9] and from the full-scale first-principle calculation [12].

IV. CONCLUSION

By performing first-principles calculations on the $6H$ -SiC surface, we have shown that the atomic structures of the unreconstructed (0001) surface have different bonding characteristics from those of the (0001) side. The electronic structures for both surfaces share a similarity in that the ground states are ferromagnetically-ordered states with energy gaps. The electronic structures of epitaxial graphene with $\sqrt{3} \times \sqrt{3}R30^\circ$ periodicity on the (0001) surface also differ from those on the (0001) surface. From the calculations so far, there are indeed differences in the atomic and the electronic structures between the systems on different sides of $6H$ -SiC{0001}. However, to understand quantitatively existing experiments [6–9] on the physical properties of epitaxial graphene on both sides of $6H$ -SiC{0001}, a calculation of the electronic structures of systems with full-scale experimental reconstructions, as was done for epitaxial graphene with $6\sqrt{3} \times 6\sqrt{3}R30^\circ$ periodicity on the $4H$ -SiC(0001) surface [12], is important

ACKNOWLEDGMENTS

Y.-W. S. was supported by the faculty research fund of Konkuk University in 2007.

REFERENCES

- [1] K. S. Novoselov, A. K. Geim, S. V. Morozov, D. Jiang, Y. Zhang, S. V. Dubonos, I. V. Grigorieva and A. A. Firsov, *Science* **306**, 666 (2004).
- [2] K. S. Novoselov, A. K. Geim, S. V. Morozov, D. Jiang, M. I. Katsnelson, I. V. Grigorieva, S. V. Dubonos and A. A. Firsov, *Nature* **438**, 197 (2005).
- [3] Y. Zhang, Y.-W. Tan, H. L. Stormer and P. Kim, *Nature* **438**, 201 (2005).
- [4] A. K. Geim and K. S. Novoselov, *Nature Mat.* **6**, 183 (2007).
- [5] A. H. Castro Neto, F. Guinea, N. M. R. Peres, K. S. Novoselov and A. K. Geim, *Rev. Mod. Phys.* **81**, 109 (2009).

- [6] C. Berger, Z. Song, X. Li, X. Wu, N. Brown, C. Naud, D. Mayou, T. Li, J. Hass, A. N. Marchenkov, E. H. Conrad, P. N. First and W. A. de Heer, *Science* **312**, 1191 (2006).
- [7] W. A. de Heer, C. Berger, X. Wu, P. N. First, E. H. Conrad, X. Li, T. Li, M. Sprinkle, J. Hass, M. L. Sadowski, M. Potemski and G. Marinez, *Solid State Commun.* **143**, 92 (2007).
- [8] A. Bostwick, T. Ohta, T. Seyller, K. Horn and E. Rotenberg, *Nat. Phys.* **3**, 36 (2007).
- [9] S. Y. Zhou, G.-H. Gweon, A. V. Fedorov, P. N. First, W. A. de Heer, D.-H. Lee, F. Guinea, A. H. Castro Neto and A. Lanzara, *Nature Mat.* **6**, 770 (2007).
- [10] A. Mattausch and O. Pankratov, *Phys. Rev. Lett.* **99**, 076802 (2007).
- [11] F. Varchon, R. Feng, J. Hass, X. Li, B. N. Nguyen, C. Naud, P. Mallet, J.-Y. Veullen, C. Berger, E. H. Conrad and L. Magaud, *Phys. Rev. Lett.* **99**, 126805 (2007).
- [12] S. Kim, J. Ihm, H. J. Choi and Y.-W. Son, *Phys. Rev. Lett.* **100**, 176802 (2008).
- [13] F. Varchon, P. Mallet, J.-Y. Veullen and L. Magaud, *Phys. Rev. B* **77**, 235412 (2008).
- [14] J. Hass, F. Varchon, J. E. Millan-Otoya, M. Sprinkle, N. Sharma, W. A. de Heer, C. Berger, P. N. First, L. Magaud, and E. H. Conrad, *Phys. Rev. Lett.* **100**, 125504 (2008).
- [15] F. Varchon, P. Mallet, L. Magaud and J.-V. Veullen, *Phys. Rev. B* **77**, 165415 (2008).
- [16] R. Kaplan, *Surf. Sci.* **215**, 111 (1989).
- [17] J. R. Ahn, S. S. Lee, N. D. Kim, C. G. Hwang, J. H. Min and J. W. Chung, *Surf. Sci.* **516**, L529 (2002).
- [18] J.-M. Themlin, I. Forbeaux, V. Langlais, H. Belkhir and J.-M. Debever, *Europhys. Lett.* **39**, 61 (1997).
- [19] M. Sabisch, P. Krüger and J. Pollmann, *Phys. Rev. B* **55**, 10561 (1997).
- [20] J. Furthmüller and F. Bechstedt, *Phys. Rev. B* **58**, 13712 (1998).
- [21] J. E. Northrup and J. Neugebauer, *Phys. Rev. B* **57**, R4230 (1998).
- [22] M. Rohlfing and J. Pollmann, *Phys. Rev. Lett.* **84**, 135 (1999).
- [23] F. Bechstedt and J. Furthmüller, *J. Phys.: Condens. Matter* **16**, S1721 (2004).
- [24] K. V. Emtsev, Th. Seyller, L. Ley, A. Tadich, L. Broekman, J. D. Riley, R. G. C. Leckey and M. Preuss, *Surf. Sci.* **600**, 3845 (2006).
- [25] T. Seyller, *Appl. Phys. A* **85**, 371 (2006).
- [26] K. V. Emtsev, Th. Seyller, L. Ley, L. Broekmann, A. Tadich, J. D. Riley, R. G. C. Leckey and M. Preuss, *Phys. Rev. B* **73**, 075412 (2006).
- [27] Y. Shibayama, H. Sato and T. Enoki, *Phys. Rev. Lett.* **84**, 1744 (2000).
- [28] P. Esquinazi, D. Spemann, R. Hohne, A. Setzer, K.-H. Han and T. Butz, *Phys. Rev. Lett.* **91**, 227201 (2003).
- [29] K. W. Lee and C. E. Lee, *Phys. Rev. Lett.* **97**, 137206 (2006).
- [30] O. V. Yazyev and L. Helm, *Phys. Rev. B* **75**, 125408 (2007).
- [31] S. Choi, B. W. Jeong, S. Kim and G. Kim, *Phys. Condens. Matter* **20**, 235220 (2008).
- [32] P. O. Lehtinen, A. S. Foster, Y. Ma, A. V. Krasheninnikov and R. M. Nieminen, *Phys. Rev. Lett.* **93**, 187202 (2004).
- [33] Y.-W. Son, M. L. Cohen and S. G. Louie, *Nature* **444**, 347 (2006).
- [34] Y.-W. Son, M. L. Cohen and S. G. Louie, *Phys. Rev. Lett.* **97**, 216803 (2006).
- [35] S. Okada and A. Oshiyama, *Phys. Rev. Lett.* **87**, 146803 (2001).
- [36] A. Gali, *Phys. Rev. B* **75**, 085416 (2007).
- [37] Y.-W. Son, M. L. Cohen and S. G. Louie, *Nano Lett.* **7**, 3518 (2007).
- [38] J. M. Soler, E. Artacho, J. D. Gale, A. Garcia, J. Junquera, P. Ordejón and D. Sánchez-Portal, *J. Phys. Condens. Matter* **14**, 2745 (2002).
- [39] J. P. Perdew and A. Zunger, *Phys. Rev. B* **23**, 5048 (1981).
- [40] D. M. Ceperley and B. J. Alder, *Phys. Rev. Lett.* **45**, 566 (1980).
- [41] N. Troullier and J. L. Martins, *Phys. Rev. B* **43**, 1993 (1991).
- [42] L. Kleinman and D. M. Bylander, *Phys. Rev. Lett.* **48**, 1425 (1982).